Anisotropic Interaction Potentials for He-Pyrrole, He-Furane and He-Thiophene from total Differential Cross Section Measurements

Ralf Schmidt*, Christian Gebauer, Olaf Klein, and Wolfhart Seidel

Physikalisch-Chemisches Institut, Justus-Liebig-Universität,
Heinrich-Buff-Ring 58, D-35392 Gießen

Z. Naturforsch. **52 a,** 317–322 (1997); received September 19, 1996

Differential cross section measurements are reported for scattering of an improved He-atomic beam by crossed beams of Pyrrole, Furane and Thiophene. The damping of the DCS diffraction oscillations is used to extract reliable anisotropic intermolecular potentials, applying the infinite order sudden approximation (IOSA).

Key words: Molecular Beams, Helium, Interaction Potentials, Aromaticity, Heterocyclic Compounds.

I. Introduction

As has been reported in [1], potentials of the interaction between He and rather anisotropic aromatic molecules can be determined from rotationally unresolved total differential cross sections (DCS), observed from the scattering of He atoms by these molecules. In consequence of our experiments with Benzene and Pyridine, molecules with a so-called *high electron density aromatic structure* such as Pyrrole, Furane and Thiophene were used to investigate their interaction potentials with Helium atoms.

Results of an infinite order sudden approximation calculation (IOSA) were fitted to the experimental DCS using a modified Hartree Fock dispersion potential (HFD) to model the atom-molecule interaction.

II. Experimental

The main configuration of the experimental equipment has already been described in detail in [1 - 3]. It is a crossed molecular beam unit with in-plane geometry and a mass-spectrometer detector rotatable around the scattering center. Two supersonic nozzle beams are crossed rectangularly. Damping of the diffraction oscillations in the DCS curves is mainly due to the anisotropy of the scattering molecules. But this damping may also be somewhat influenced

a) by the geometry of the scattering volume, defined by the angular divergence of both molecular beams;

b) by undesired components in the molecular beams, such as dimers;

c) by the geometry of inspection of the detector system.

Since the anisotropy (less symmetry) of the 5-ring aromates is more pronounced compared to the systems HeC_6H_6 or HeC_5H_5N, the primary He beam had to be improved appreciably. This was achieved by means of diminished cross sections of the nozzle, the skimmer and the collimator, and enhanced nozzle pressure. Consequently pumping of the whole primary beam section was to be improved (Figure 1). Nozzle and skimmer could be adjusted separately by an arrangement of 5 stepper motors. A He-Ne laser tube was used for adjustment control.

After the improvement of the primary beam section, the experimental quality of the whole equipment was tested by means of the well known scattering system He-Ar [4 - 6], which is a reliable testing method. In comparison with experimental data obtained before the improvement [1], no significant change in the He-Ar results was observed. Beam conditions of the primary beam and the parameters of the secondary beams are given in Table 1.

Since an adiabatic expansion occurs in the generation of a nozzle beam, the formation of clusters may generally be expected. To which extent cluster condensation occurs depends considerably on the polarizability of the molecules and on the nozzle pressure. In the range of the He source pressure, the formation

* Part of the Dissertation.

Reprint requests to Prof. Dr. W. Seidel.

0932-0784 / 97 / 0400-0317 $ 06.00

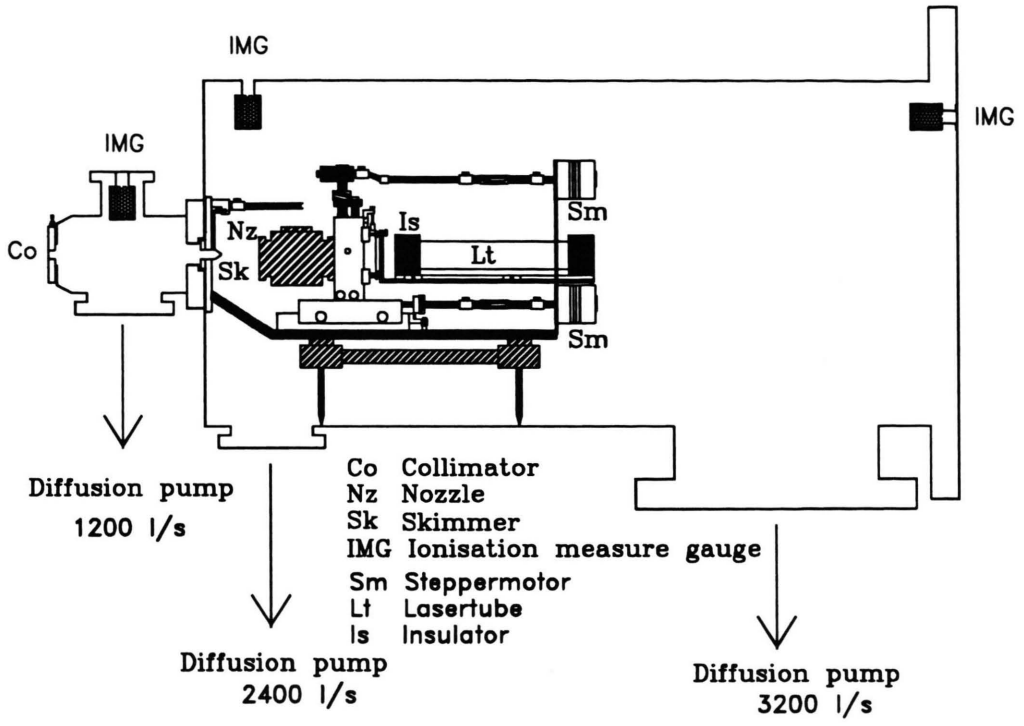

Fig. 1. Schematic view of the improved He beam source.

Table 1. Beam conditions.

Gas	Helium	Pyrrole	Furane	Thiophene
Gas purity (%)	99.996	~ 96	> 99	> 99
Nozzle pressure (bar)	45	0.1	0.1	0.08
Nozzle diameter (μm)	20	100	100	100
Nozzle temperature (K)	303	363	343	352
Skimmer diameter (mm)	0.3	0.5	0.5	0.5
Nozzle-skimmer distance (mm)	20	2.0	2.0	2.0
Collimator diameter (mm)	1.0	—	—	—
Angular divergence (degree)	0.9	6.3	7.3	7.4
most probable velocity v_{mp} (m/s)	1645	662	627	576
velocity FWHM $\Delta v/v_{mp}$	0.043	0.4	0.26	0.36
Speed ratio S	40	4.1	5.8	4.4
Collision energy (meV)	—	60.5	60.5	60.1

of clusters is not to be expected for the primary beam. Therefore only secondary beams were examined with an indirect method. Clustered molecules do not only show different signals in the mass spectrum but they are also responsible for a different time of flight (TOF) spectrum than is expected for the lighter monomeres. A sufficient number of clusters in a beam causes the corresponding TOF-peak to be widened. The width of the TOF peak serves (among other details) to calculate the speed ratio of a molecular beam [7]. Thus, the speed ratio itself can be used as a qualitative criterium for cluster formation: It appreciably decreases when clusters contribute to the beam.

Table 2. Speed ratio measurements as a function of the nozzle pressure.

Pyrrole		Furane		Thiophene	
Nozzle pressure [mbar]	Speed ratio	Nozzle pressure [mbar]	Speed ratio	Nozzle pressure [mbar]	Speed ratio
200	4.0	400	1.9	150	1.4
150	4.3	300	2.3	100	3.6
100	4.1	200	5.8	80	4.4
55	4.1	100	5.8	50	4.0

Results of speed ratio observations for different nozzle pressures are shown in Table 2. In the investigated range of the nozzle pressure no change of the speed ratio was found for Pyrrole. Thus, cluster

Table 3. Experimental total cross section measurements; experimental DCS measurements $I(\theta)$ and standard deviations $\Delta I(\theta)$ are in arbitrary units.

	He-Furane			He-Thiophene			He-Pyrrole	
θ	$I(\theta)$	$\Delta I(\theta)$	θ	$I(\theta)$	$\Delta I(\theta)$	θ	$I(\theta)$	$\Delta I(\theta)$
2.0	10000.0	248.84	2	10000.0	457.31	2	10000.0	268.69
2.5	5025.02	127.87	2.5	5105.17	102.04	2.5	5318.97	104.47
3.0	3339.38	81.15	3	3565.74	56.28	3	3852.91	65.94
3.5	2852.86	83.08	3.5	3117.21	28.40	3.5	3296.08	48.09
4.0	2470.97	56.19	4	2625.44	25.30	4	2688.43	56.32
4.5	1774.35	47.00	4.5	1826.85	29.40	4.5	1779.62	32.39
5.0	1071.96	28.84	5	1077.63	11.43	5	1042.43	23.93
5.5	654.26	16.82	5.5	657.35	13.41	5.5	693.13	13.33
6.0	563.42	12.29	6	631.30	3.92	6	692.51	11.71
7.0	601.15	14.58	6.5	680.74	8.13	6.5	736.55	8.47
7.5	511.59	10.95	7	641.67	5.90	7	655.76	11.42
8.0	365.06	9.07	7.5	492.43	6.16	7.5	499.07	6.65
8.5	233.25	7.54	8	325.28	5.37	8	332.98	7.42
9.0	166.42	6.77	8.5	217.71	7.63	8.5	238.45	7.63
9.5	160.04	4.34	9	177.96	4.12	9	201.61	5.86
10.0	169.10	2.67	9.5	175.58	4.80	9.5	198.90	4.82
10.5	171.24	4.51	10	184.35	3.59	10	190.83	5.03
11.0	151.12	4.05	10.5	171.53	3.39	10.5	167.81	3.43
11.5	124.22	4.16	11	129.50	2.85	11	141.82	3.92
12.0	94.53	2.59	11.5	104.73	3.23	11.5	116.38	3.97
12.5	82.30	2.56	12	83.23	3.13	12	91.13	4.24
13.0	78.28	3.06	12.5	84.40	3.06	12.5	88.65	2.10
13.5	76.09	2.19	13	80.40	3.13	13	85.13	3.68
14.0	67.47	2.94	13.5	73.61	3.71	13.5	74.44	3.48
14.5	63.10	1.83	14	60.11	4.67	14	69.93	3.17
15.0	55.07	2.52	14.5	53.89	1.89	14.5	58.82	2.44
15.5	50.52	2.23	15	42.85	3.69	15	59.30	7.41
16.0	45.56	1.77	15.5	42.27	2.33	15.5	50.17	1.44
16.5	43.99	2.04	16	39.66	3.39	16	45.78	1.91
17.0	41.49	1.91	16.5	40.53	3.14	16.5	45.61	3.36
17.5	41.87	1.57	17	43.42	2.38	17	44.30	2.38
18.0	37.58	1.43	17.5	35.24	2.64	17.5	35.59	2.43
18.5	37.45	2.02	18	29.79	1.59	17.9	33.99	1.8

formation is assumed to be negligible. Contrary to Pyrrole, the speed ratio for Furane and Thiophene is drastically lowered above a nozzle pressure of 100 mbar, thus indicating reinforced formation of clusters. The result for Thiophene confirms measurements from other authors [8].

III. Analysis

A) Intermolecular potential

The experimental DCS data were analyzed by applying the IOSA [9 - 12] based on a modified form of Aziz et al. [13]. For the isotropic part of the interactions we used the HFD potential as follows:

$$V(R) = \varepsilon \cdot f(R), \tag{1}$$

$$f_{\text{rep}}(r) = a \cdot \exp[-b \cdot (r - 1)], \tag{2}$$

$$f_{\text{att}}(r) = -\left(\frac{c_6}{r^6} + \frac{c_8}{r^8} + \frac{c_{10}}{r^{10}}\right), \tag{3}$$

$$d(r) = \begin{cases} \exp\left[-\left(\frac{1.28}{r} - 1\right)^2\right] & \text{for } r \geq 1.28, \\ 1 & \text{for } r \leq 1.28. \end{cases} \tag{4}$$

All constants were used in a reduced form:

$$r = R/R_m, \tag{5}$$

$$c_n = C_n/R_n^m \varepsilon_m, \tag{6}$$

$$a = A/\varepsilon_m. \tag{7}$$

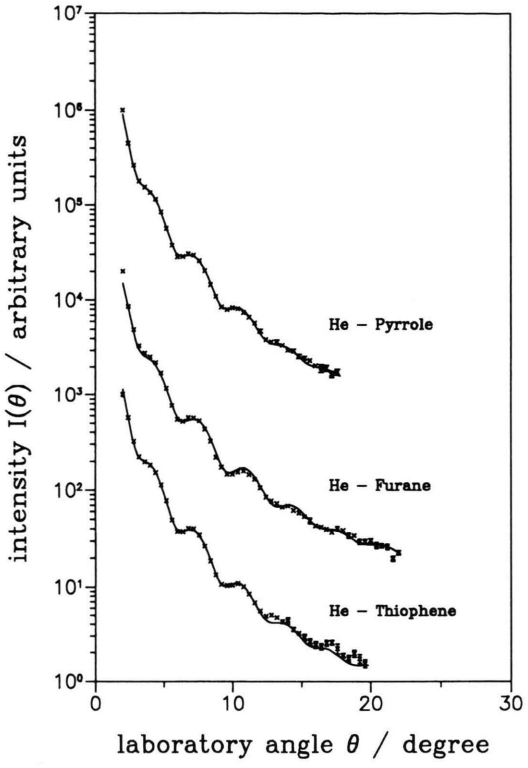

Fig. 2. Laboratory differential cross sections for the scattering of He by Pyrrole, Furane and Thiophene, respectively. The ordinates are shifted arbitrarily. Points with error-bars are experimental measurements of the total differential cross section. Solid lines are calculated using potentials extracted from the experimental data.

For c_{10}, one of the combination rules of Douketis [14] was used:

$$c_{10} \approx 1.225 \frac{c_8^2}{c_6}. \tag{8}$$

Furthermore, the parameters a and b are fixed by the minimum of the potential:

$$a = 0.9246(c_6 + c_8 + c_{10}) - 1, \tag{9}$$

$$b = \frac{5.2832c_6 + 7.2832c_8 + 9.2832c_{10}}{c_6 + c_8 + c_{10} - 1.0816}. \tag{10}$$

However, the molecules under investigation deviated considerably from isotropy, so certain anisotropic contributions were to be added. Therefore ε_m and R_m were expanded by means of *Legendre-polynomials* according to the symmetry of the molecules under investigation.

The oblate shape of the scattering molecules was taken into account by

$$P_2 = (3\cos^2(\theta) - 1)/2, \quad \theta : \text{polar angle (Figure 3).} \tag{11}$$

The "five-fold" symmetry in the equatorial plane was modelled by

$$P_5 = -21\cos(5\phi)\sin^5(\theta)/32, \quad \phi : \text{angle in the equatorial plane (Figure 3).} \tag{12}$$

As a consequence, the following energy and radius parameter was used, respectively:

$$\varepsilon_m = E_0 + P_2E_2 + P_5E_5, \tag{13}$$

$$R_m = R_0 + P_2R_2 + P_5R_5. \tag{14}$$

B) Data Analysis and Fitting

To analyze the DCS data, the IOSA [9 - 12] was used. DCS were calculated for various spatial orientations (θ, ϕ) by partial wave analysis using phase shifts from the semiclassical *Jeffreys-Wentzel-Kramers-Brillouin* (JWKB) approximation as modified by Langer [15]. Scattering phase shifts were calculated applying a ten-point *Gauß-Mehler* quadrature [16]. According to the IOS formula

$$I(\vartheta) = \frac{1}{4\pi}\int_0^{2\pi}\int_0^{\pi} |f(\vartheta, \theta, \phi)|^2 \sin\theta \, \mathrm{d}\theta \, \mathrm{d}\phi, \tag{15}$$

where ϑ describes the scattering angle, the DCS were averaged with respect to θ and ϕ [17] by means of two 16-point *Gauß-Legendre* quadratures.

In order to compare calculated DCS data with our experimental results, the calculated data were to be transformed from the center-of-mass system to the laboratory system. This transformation was performed using the elastic *Jacobian*. Transformed data were averaged with respect to the angular and velocity distributions of both beams, and with respect to the finite aperture of the detector as described in [18].

IV. Results and Discussion

The total cross sections of the investigated scattering systems are listed in Table 3. Figure 2 shows

Table 4. Best-fit potential parameters.

Parameter	He-Pyrrole	He-Furane	He-Thiophene
E_0 [meV]	4.39	4.57	4.65
E_2 [meV]	2.59	2.92	1.99
E_5 [meV]	2.43	1.43	1.57
R_0 [pm]	442	435	453
R_2 [pm]	–69	–60	–68
R_5 [pm]	18	26	14
c_6	1.38	1.34	1.47
c_8	0.44	0.35	0.46
c_{10}	0.18	0.11	0.17
A	0.85	0.66	0.94
B	13.22	14.86	12.48
$E_\parallel$ [meV]	1.42	2.12	2.57
$E_\perp$ [meV]	5.38	6.55	5.60
$R_\parallel$ [pm]	464	447	476
$R_\perp$ [nm]	361	358	374

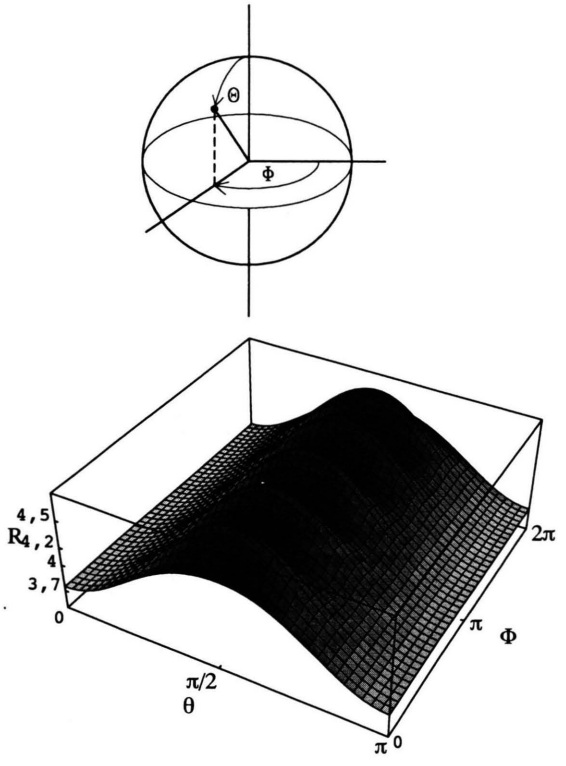

Fig. 3. Energy surface of the interaction potential He-Furane.

measured and calculated DCS results; the latter were obtained using the best fit parameter set for the respective potential (Table 4).

Compared to an isotropic scattering system, e. g. He-Ar, appreciable damping of the diffraction oscillation is observed, as was to be expected. This is due to the anisotropy of the target molecules. Although it can be assumed that the rings have a flat structure, the observable diffraction oscillations of the scattering curve indicate that the He atom in this case is able to detect a nearly isotropic part of the potential. If furthermore the parameters $E_\parallel$ and $E_\perp$, $R_\parallel$ and $R_\perp$ from Table 4 are taken into account, which represent the properties of the interaction potentials for $\theta = 90°(\parallel)$ and $\theta = 0°(\perp)$ (Fig. 3), it is obvious that the interaction energy perpendicular to the equatorial plane, $E_\perp$, is up to 4 times that of the corresponding $E_\parallel$. Considering that each of the target molecules possesses an aromatic system of 6 π-electrons with appreciable density above and below the ring plane, this result appears to be plausible. The value of the parameter R_2 which is responsible for the oblate structure of the ring molecules is only about 100 pm. Taking into account that the respective isotropic parameter R_0 has a value of about 450 pm, one may realize that there is no marked anisotropy perpendicular to the ring plane, with respect to the radius parameter.

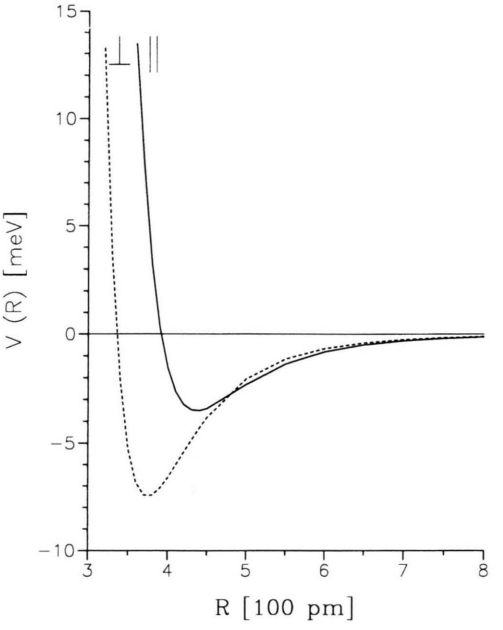

Fig. 4. Hartree-Fock-Dispersion function for both orientations, perpendicular and parallel, of the He-atom towards the Furane molecule.

Moreover, the relative small difference between $R_\perp$ and $R_\parallel$ gives evidence for this fact. Figure 4 shows the HFD potential curve for two spatial orien-

tations, ($\theta = 0°$, marked $\perp$, and $\theta = 90°$, marked $\|$) of a Helium atom approaching a Furane molecule.

One aim of the present investigation was to observe whether or not any anisotropy in the ring plane of the target molecules can be detected. As a result, anisotropy of the energy can clearly be recognized from E_5, ranging between E_0 and E_2. This is presented in a 3D plot of the potentials for the system He-Furane (Figure 3). The energies are pictured in different grey colours on the resulting net in which a darker grey represents stronger interactional energy in general.

However, the results are very similar for the two other scattering systems. Therefore additional plots are omitted. Due to the similarity of the aromatic systems, the E_2 data for all three scattering systems are almost equal. Contrary to this result, the interaction energies in the ring plane, $E_{\|}$, show significant differences. Especially the value for He-Pyrrole deviates considerably from those of the other molecules. This may be explained by the increased σ electron density in the ring plane of Thiophene and Furane, since the S and O atoms respectively contribute an additional pair of electrons.

Acknowledgement

Support by the "Fonds der Chemischen Industrie", the "Hoechst AG-Werk Cassella" and the "Deutsche Forschungsgemeinschaft" is gratefully acknowledged.

[1] R. Brandt, M. Henkel, B. Pfeil, and W. Seidel, J. Chem Phys. **95**, 135 (1991).
[2] M. Henkel, B. Pfeil, and W. Seidel, J. Chem Phys. **96**, 5054 (1992).
[3] R. Schmidt, Dissertation, Justus-Liebig-Universität Gießen 1996.
[4] L. J. Danielson and M. Keil, J. Chem. Phys. **88**, 851 (1988).
[5] K. M. Smith, A. U. Rulis, G. Scoles, R. A. Aziz, and V. Nain, J. Chem. Phys. **67**, 152 (1977).
[6] C. H. Chen, P. E. Siska, and Y. T. Lee, J. Chem. Phys. **59**, 601 (1973).
[7] Ch. Gebauer, Dissertation, Justus-Liebig-Universität, Gießen 1996.
[8] E. A. Walters, J. R. Grover, T. J. Clay, P. Cid-Aguero and M. V. Wilcox, Phys. Chem. **96**, 7236 (1992).
[9] G. A. Parker and R. T. Pack, J. Chem. Phys. **68**, 1585 (1978).
[10] U. Buck, V. Khare, und M. Kick, Mol. Phys. **35**, 65 (1978).
[11] R. T. Pack, Chem. Phys. Lett. **55**, 197 (1979).
[12] G. Rotzoll and A. Lübbert, J. Chem. Phys. **71**, 2275 (1979).
[13] R. A. Aziz, P. W. Riley, U. Buck, G. Maneke, J. Schleusener, G. Scoles, and U. Valbusa, J. Chem. Phys. **71**, 2637 (1979).
[14] C. Douketis, G. Scoles, S. Marchetti, M. Zen, and A. J. Thakkar, J. Chem. Phys. **76**, 3057 (1982).
[15] R. E. Langer, Phys. Rev. **51**, 669 (1937).
[16] J. S. Cohen, J. Chem. Phys. **68**, 1841 (1978).
[17] R. T. Pack, J. Chem. Phys. **60**, 633 (1979).
[18] M. Henkel, Dissertation, Justus-Liebig-Universität, Gießen 1991.